

Thermal Conductivity and Interfacial Thermal Resistance: Measurements of Thermally Oxidized SiO₂ Films on a Silicon Wafer Using a Thermo-Reflectance Technique

Ryozo Kato · Ichiro Hatta

Published online: 15 November 2008
© Springer Science+Business Media, LLC 2008

Abstract This article describes the development of a method to measure the normal-to-plane thermal conductivity of a very thin electrically insulating film on a substrate. In this method, a metal film, which is deposited on the thin insulating films, is Joule heated periodically, and the ac-temperature response at the center of the metal film surface is measured by a thermo-reflectance technique. The one-dimensional thermal conduction equation of the metal/film/substrate system was solved analytically, and a simple approximate equation was derived. The thermal conductivities of the thermally oxidized SiO₂ films obtained in this study agreed with those of VAMAS TWA23 within $\pm 4\%$. In this study, an attempt was made to estimate the interfacial thermal resistance between the thermally oxidized SiO₂ film and the silicon wafer. The difference between the apparent thermal resistances of the thermally oxidized SiO₂ film with the gold film deposited by two different methods was examined. It was concluded that rf-sputtering produces a significant thermal resistance ($(20 \pm 4.5) \times 10^{-9} \text{ m}^2 \cdot \text{K} \cdot \text{W}^{-1}$) between the gold film and the thermally oxidized SiO₂ film, but evaporation provides no significant interfacial thermal resistance (less than $\pm 4.5 \times 10^{-9} \text{ m}^2 \cdot \text{K} \cdot \text{W}^{-1}$). The apparent interfacial thermal resistances between the thermally oxidized SiO₂ film and

R. Kato
Ulvac-Riko Inc, 1-9-19 Hakusan, Midoriku, Yokohama 226-0006, Japan

I. Hatta
Fukui University of Technology, 3-6-1 Gakuen, Fukui 910-0028, Japan

Present Address:

R. Kato (✉)
National Institute for Materials Science, 1-2-1 Sengen, Tsukuba, Ibaraki 305-0047, Japan
e-mail: Kato.ryozo@nims.go.jp; rkato@aqua.ocn.ne.jp

I. Hatta
Industrial Application Division, Japan Synchrotron Radiation Research Institute,
SPring-8, 1-1-1 Kouto, Sayo, Hyogo 679-5198, Japan

the silicon wafer were found to scatter significantly ($\pm 9 \times 10^{-9} \text{ m}^2 \cdot \text{K} \cdot \text{W}^{-1}$) around a very small thermal resistance (less than $\pm 4.5 \times 10^{-9} \text{ m}^2 \cdot \text{K} \cdot \text{W}^{-1}$).

Keywords Interfacial thermal resistance · Periodic method · Thermal conductivity · Thermally oxidized SiO₂ film · Thermo-reflectance

Nomenclature

$T(0)$	ac temperature of the surface of the metal film, K
T_{AC}	In-phase amplitude of the ac-temperature of the surface of the metal film, K
q	ac-power per unit volume, $\text{W} \cdot \text{m}^{-3}$
ω	Angular frequency, s^{-1}
k	Wave number, m^{-1}
d	Thickness, m
λ	Thermal conductivity, $\text{W} \cdot \text{m}^{-1} \cdot \text{K}^{-1}$
C	Specific heat capacity per unit volume, $\text{J} \cdot \text{m}^{-3} \cdot \text{K}^{-1}$
R	Thermal resistance, $\text{m}^2 \cdot \text{K} \cdot \text{W}^{-1}$
Subscripts _{0,1,S}	Denote metal film layer, thin filmlayer, and substrate layer, respectively

1 Introduction

The microelectronics industry requires techniques for measuring the thermal conductivity of electrically insulating materials in the form of very thin films deposited on a substrate to evaluate heat dissipation across the thin films to a substrate. We have developed an advanced method to measure the normal-to-plane thermal conductivity of a very thin insulating film. In this method, a metal film deposited on the thin-film specimen is Joule heated periodically, and the ac-temperature response at the center of the metal film surface is measured by a thermo-reflectance technique. Thus, the one-dimensional model can be applied to the thermal system. The one-dimensional thermal conduction equation was solved analytically, and a simple approximate equation was derived. This method requires very simple specimen preparation in comparison with the three-omega method [1]. This method has been verified by thermal-conductivity measurements of thermally oxidized SiO₂ films on a silicon wafer [2–4]. In this article we corrected a mathematical error found in the principal equation, which has been used in our previous study. According to the corrected equation, we recalculated the thermal conductivities from the same experimental data, which have been used in our previous study [4]. As a result, these data show much improved agreement over those of VAMS TWA23 (NIST Round Robin Report) [5,6].

In this study we also tried to determine the interfacial thermal resistance between the thermally oxidized SiO₂ film and a silicon wafer separately, although by this method we can measure only the total interfacial thermal resistance, which includes the interfacial thermal resistance between the gold film and the thermally oxidized SiO₂ film, and that between the thermally oxidized SiO₂ film and the silicon wafer.

We examined the difference between the apparent thermal resistances of the thermally oxidized SiO₂ film on which the gold film is deposited by two different methods. One of them is rf-sputtering, and the other is evaporation.

2 Theoretical Considerations

The thermal-conductivity measurement system of this method is shown schematically in Fig. 1. As shown in the figure, it consists of three layers, which are the metal film layer, the thin-film layer, and the substrate layer. The metal film is Joule heated periodically, and the ac-temperature response at the center of the metal-film surface is measured by a thermo-reflectance technique. Although the metal film is ac-heated uniformly, an ac-temperature gradient across the thickness of the metal film layer may take place. It is assumed that the substrate layer has infinite thickness, but the metal film layer and the thin film layer have finite thicknesses. The one-dimensional thermal conduction equation of the system in the normal-to-plane direction was solved analytically. When the following conditions are valid,

$$k_0 d_0 \ll 1 \quad (1a)$$

$$k_1 d_1 \ll 1 \quad (1b)$$

the solution of the thermal conduction equation can be simplified to the following equation,

$$\frac{T(0)}{q d_0} = \frac{\exp\left(-\frac{\pi}{4}i\right)}{\sqrt{\lambda_S C_S \omega}} + \left(1 - \frac{\lambda_1 C_1}{\lambda_S C_S}\right) \frac{d_1}{\lambda_1} + \left(\frac{1}{2} - \frac{\lambda_0 C_0}{\lambda_S C_S}\right) \frac{d_0}{\lambda_0} \quad (2)$$

where q denotes the heat per unit volume and d_0 and d_1 denote the thicknesses of the metal film layer and the thin film layer, respectively. In Eq. 2, we have made a correction for the mathematical error found in the second term of the equation, which has been used in our previous study ([4], Y. Xu, private communication, 2006). By taking only the real part of Eq. 2, the following equation is found:

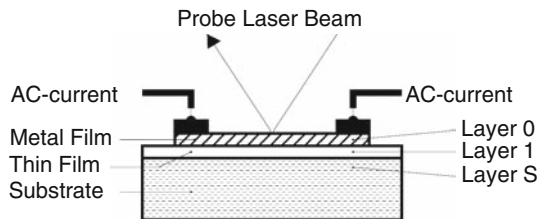


Fig. 1 The thermal conductivity measurement system of this method consists of three layers, which are the metal film layer, the thin film layer, and the substrate layer. The metal film is Joule heated periodically and the ac-temperature response at the center of the metal film surface is measured by a thermo-reflectance technique. Thus, a one-dimensional model can be applied to the thermal system

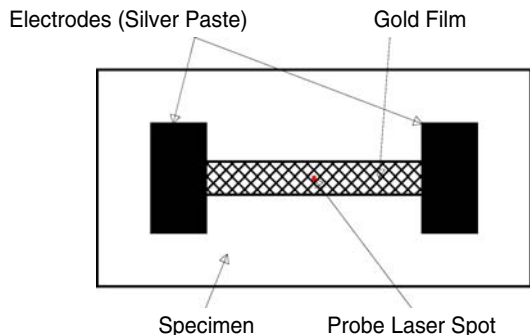
$$\frac{T_{AC}}{qd_0} = \frac{1}{\sqrt{2\lambda_S C_S \omega}} + \left(1 - \frac{\lambda_1 C_1}{\lambda_S C_S}\right) \frac{d_1}{\lambda_1} + \left(\frac{1}{2} - \frac{\lambda_0 C_0}{\lambda_S C_S}\right) \frac{d_0}{\lambda_0} \quad (3)$$

where T_{AC} denotes the in-phase amplitude of the ac-temperature response. The first term on the right-hand side of Eq. 3 is proportional to $\omega^{-1/2}$, and the factor of proportionality is $(2\lambda_S C_S)^{-1/2}$. On the other hand, the second and third terms of Eq. 3 are constants independent of $\omega^{-1/2}$. So the T_{AC}/qd_0 versus $\omega^{-1/2}$ plot for Eq. 3 gives a slope-intercept form. The slope is strictly related to the factor of proportionality and the intercept to the sum of the second and third terms. The second and third terms correspond to the apparent thermal resistances of the thin film and the metal film, respectively. To determine the absolute value of the thermal conductivity of a thin film, the calibration factor of the thermo-reflectance coefficient must be known. In this method, the calibration factor of the thermo-reflectance coefficient is determined by fitting the experimentally obtained slope with the factor of proportionality, which can be calculated theoretically using the known thermophysical properties (thermal effusivity $\lambda_S C_S$) of the substrate. It should be noted here that the factor of proportionality is only a function of the thermophysical properties of the substrate layer, but not that of other layers. Actually, the calibration factor includes the error corrections for the measurement of the ac power per unit area supplied to the metal-film heater, making the application of the method much easier.

3 Experimental

In the experimental system, the specimen is set horizontally on the sample stage. The thermoelectric cooler (TEC) system keeps the sample stage at a constant temperature (25 °C). The whole sample assembly is installed in a vacuum chamber. At the top of the chamber above the sample assembly, an optical window is provided to enable thermo-reflectance measurements. As shown in Fig. 2, the size of the specimen is 20 mm × 10 mm. The metal film is stripe-shaped with dimensions of 1.7 mm width, 10 mm length, and 100 nm thickness. The metal film is deposited on the specimen by rf-sputtering (Ulvac-Kiko, Model RFS-200) or evaporation using a mask. At both ends of the metal film, a pair of electrodes made of silver paste is painted to make good electrical contact with the spring contactors for supplying an ac current.

Fig. 2 Size of the specimen is 20 mm × 10 mm. Metal film is stripe-shaped with dimensions of 1.7 mm width, 10 mm length, and 100 nm thickness. The metal film is deposited on the specimen by rf-sputtering or evaporation using a mask



The differential optical system minimizes the effect of the common-mode noise of the HeNe laser [7]. The signal-to-noise ratio of the optical system is less than 0.02 ppm (at 500 Hz). In the case of the gold film sensor, the temperature-equivalent noise of the system is less than 3×10^{-4} K. As the amplitude of the ac-temperature response is several 0.1 K, the dynamic range of the system is several hundreds. The photocurrent signal of the differential-photodiode sensor is fed into the lock-in amplifier to measure the second harmonic of the signal. The frequency range available in the system is from 500 Hz to 8,000 Hz.

To ensure an uncertainty of $\pm 0.1\%$ with Eq. 3, the frequency must be in the range as discussed below. For the case when a silicon substrate with a thickness of 0.5 mm is used, the frequency must be higher than 500 Hz to minimize the effect of the temperature waves reflected at the bottom of the substrate. For the case when a gold film sensor with a thickness of 100 nm is used, the frequency must be lower than 2 MHz to satisfy Eq. 1a. For measurements of the thermally oxidized SiO₂ films with a thickness less than 1,000 nm, the frequency must be lower than 8,000 Hz to satisfy Eq. 1b. The thermal conductivity of the gold film was determined by the ac-calorimetric method [8]. For the case when a gold film sensor is used with a silicon substrate, the apparent thermal resistance of the gold film layer is negligibly small ($\pm 0.5 \times 10^{-9} \text{ m}^2 \cdot \text{K} \cdot \text{W}^{-1}$) in comparison with that of the thermally oxidized SiO₂ films.

4 Results and Discussion

In this study, the results for the thermal conductivities of the thermally oxidized SiO₂ films on a silicon wafer were obtained by recalculating them from the same experimental data used in our previous study [4]. So the condition of the specimen and the values of thermophysical properties are the same as those used in our previous study. Figures 3 and 4 show a T_{AC} (in-phase amplitude)/ qd_0 versus $\omega^{-1/2}$ plot of the thermal conductivity measurements of the thermally oxidized SiO₂ films on a silicon wafer (NIST RR and KST samples, respectively). In these measurements, the gold film was deposited on the specimen by rf-sputtering. In Figs. 3 and 4, many dataset are plotted together showing the reproducibility of the measurements at each frequency for the same piece of the specimen. The results of the thermal conductivities obtained from the coefficient of the straight-line fit for the apparent thermal resistance versus thickness plot (NIST RR and KST samples) are listed in Table 1 together with literature data including our previous data [4]. In Table 1 the uncertainties of these data were estimated from the standard deviation of the coefficients of the straight-line fits. These results of the thermal-conductivity measurements agree with those of VAMAS TWA23 within $\pm 4\%$ [5,6].

To determine the interfacial thermal resistance between the thermally oxidized SiO₂ film and the silicon wafer, we tried to examine the apparent thermal resistance of the thermally oxidized SiO₂ film with a thickness of 20 nm, assuming that the thermally oxidized SiO₂ film is uniformly grown on the silicon wafer. The silicon wafer on which the thermally oxidized SiO₂ film is grown is a p-type [100] single crystal. The sample was supplied by KST Corporation. Several pieces were randomly sampled as shown in Fig. 5 and deposited with a gold film by two different methods

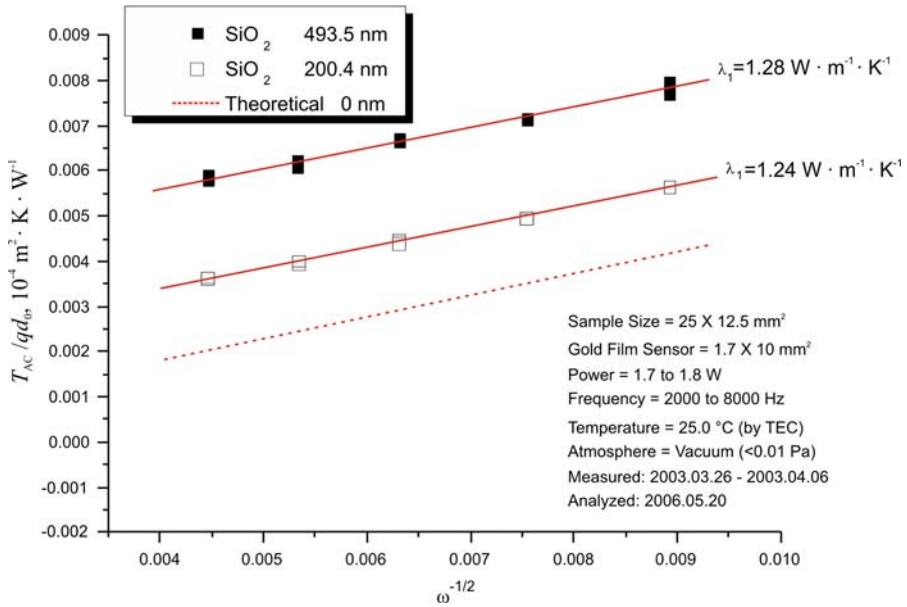


Fig. 3 T_{AC} (in-phase amplitude)/ $q d_0$ versus $\omega^{-1/2}$ plots of the thermal-conductivity measurements of the thermally oxidized SiO_2 films on a silicon wafer (NIST RR samples)

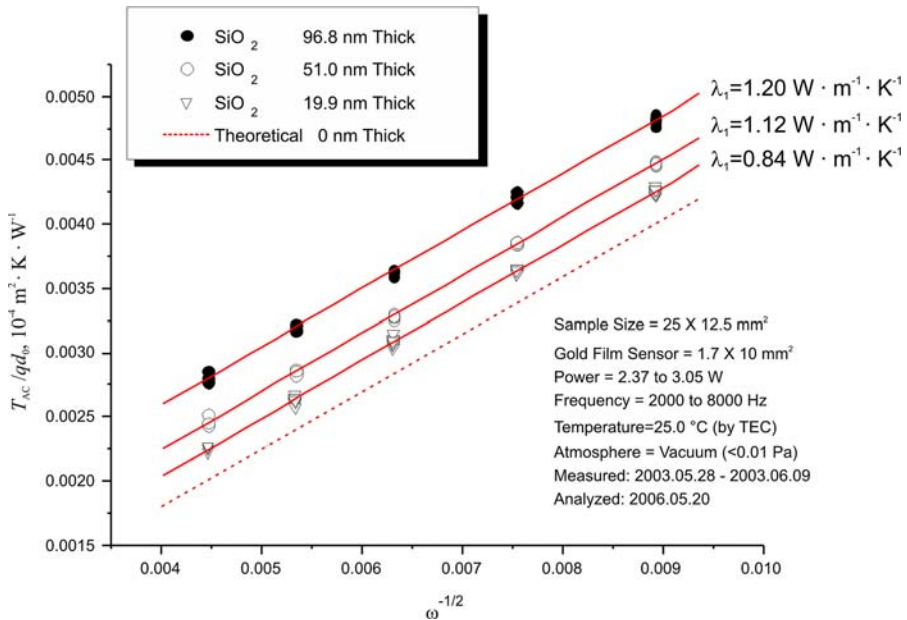
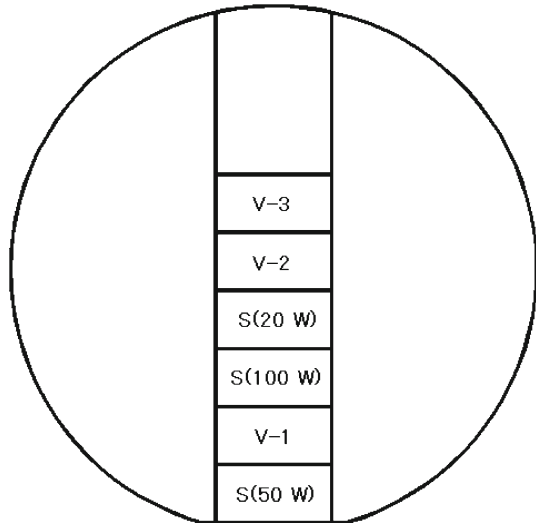


Fig. 4 T_{AC} (in-phase amplitude)/ $q d_0$ versus $\omega^{-1/2}$ plots of thermal-conductivity measurements of the thermally oxidized SiO_2 films on a silicon wafer (KST samples)

Table 1 Results of the thermal conductivities of thermally oxidized SiO₂ films on a silicon wafer obtained from the coefficient of the straight-line fit for the apparent thermal resistance versus thickness plot

	VAMAS TWA23 data obtained by the three-omega method (50 nm to 500 nm thick NIST RR samples) [5,6]	Data obtained by this method (200 nm to 500 nm thick NIST RR samples)	Data obtained by this method (20 nm to 100 nm thick KST samples)
λ_1 (W · m ⁻¹ · K ⁻¹)	1.38 ± 0.05	1.32 ± 0.04 1.21 ± 0.04 ^a	1.35 ± 0.04 1.24 ± 0.04 ^a

^a These data were obtained in our previous study [4]

Fig. 5 Several pieces were randomly sampled from a single silicon wafer on which the thermally oxidized SiO₂ film is grown (KST sample)

[9]. Three pieces of the samples were deposited with the gold film by rf-sputtering, and the other three pieces by evaporation. The thickness distribution of the thermally oxidized SiO₂ film was measured with an ellipsometer, and its scatter was less than ±0.2 nm. Surface roughness was also measured to be less than 2 nm by an atomic force microscope (AFM) as shown in Fig. 6. So the scatter of the apparent thermal resistances due to the scatter of the thickness or the surface roughness will not exceed $\pm 1.4 \times 10^{-9} \text{ m}^2 \cdot \text{K} \cdot \text{W}^{-1}$.

Results of the apparent thermal resistances are listed in Table 2. It shows that the apparent thermal resistance yielded by rf-sputtering is about $(20 \pm 4.5) \times 10^{-9} \text{ m}^2 \cdot \text{K} \cdot \text{W}^{-1}$ greater than that by evaporation. This value is almost the same as the total interfacial thermal resistance reported in VAMAS TWA23, where sputtering was mainly used for deposition of the metal film [5,6].

The total interfacial thermal resistances were obtained by subtracting the values of the second and third terms of Eq. 3, assuming that a very thin interfacial region (<20 nm) of the thermally oxidized SiO₂ film has the same thermal conductivity as

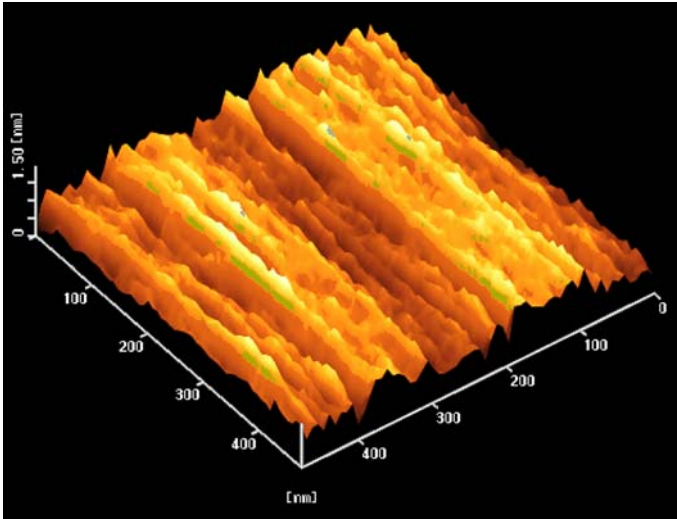


Fig. 6 Surface roughness of the thermally oxidized SiO₂ film on a silicon wafer (KST sample) measured by an atomic force microscope (AFM)

Table 2 Results of the apparent thermal resistances of thermally oxidized SiO₂ film on a silicon wafer (20 nm thick KST sample) with the gold film deposited by rf-sputtering and evaporation

Method of the deposition	Date of the deposition	Date of the measurements	Apparent thermal resistances (10 ⁻⁹ m ² · K · W ⁻¹)
Rf-sputtering S (20 W) ^a	2004/8	2004/8	36.85 ± 4.05
Rf-sputtering S (50 W) ^a	2003/6	2003/6	23.33 ± 1.54
		2004/8	22.90 ± 7.12
Rf-sputtering S (100 W) ^a	2004/8	2004/8	37.58 ± 4.05
Rf-sputtering (mean)			32.7 ± 8.0
Evaporation (V-1)	2004/8	2004/8	17.61 ± 1.68
Evaporation (V-2)	2004/8	2004/8	-0.81 ± 4.79
Evaporation (V-3)	2004/8	2004/8	7.83 ± 1.66
Evaporation (mean)			8.2 ± 9.2
Difference between rf-sputtering and evaporation (mean)			24.3 ± 4.5

^a Sputtering power is shown in each case

that determined for the thickness range from 20 nm to 500 nm. The values ((14.2 ± 1.4) × 10⁻⁹ m² · K · W⁻¹ and (-0.4 ± 0.1) × 10⁻⁹ m² · K · W⁻¹, respectively) were calculated using known thermophysical properties including the thermal conductivity of the thermally oxidized SiO₂ film determined in this study and are listed in Table 1.

Defining R_S , R_V , and R_I as follows, Eqs. 4 and 5 are valid with uncertainties of ±9 × 10⁻⁹ m² · K · W⁻¹ and ±4.5 × 10⁻⁹ m² · K · W⁻¹, respectively. R_S is the

Table 3 Results of the interfacial thermal resistances between the thermally oxidized SiO₂ film and the silicon wafer

	VAMAS TWA23 data obtained by three-omega method (50 nm to 500 nm thick NIST RR samples)	Data obtained by this method (20 nm thick KST sample)
Interfacial thermal resistance, R_I ($10^{-9} \text{ m}^2 \cdot \text{K} \cdot \text{W}^{-1}$)	2.9 ± 8.8^a	-3.5 ± 8.6

^a Data were corrected by subtracting the interfacial thermal resistance R_S estimated in this study from the original data ($(22.9 \pm 8.8) \times 10^{-9} \text{ m}^2 \cdot \text{K} \cdot \text{W}^{-1}$) [5,6]

interfacial thermal resistance ($10^{-9} \text{ m}^2 \cdot \text{K} \cdot \text{W}^{-1}$) between the rf-sputtered gold film and the thermally oxidized SiO₂ film, R_V is the interfacial thermal resistance ($10^{-9} \text{ m}^2 \cdot \text{K} \cdot \text{W}^{-1}$) between the evaporated gold film and the thermally oxidized SiO₂ film, and R_I is the interfacial thermal resistance ($10^{-9} \text{ m}^2 \cdot \text{K} \cdot \text{W}^{-1}$) between the thermally oxidized SiO₂ film and the silicon wafer.

$$R_S + R_I = 20 \quad (4)$$

$$R_V + R_I = 0 \quad (5)$$

According to the conditions of $R_V \geq 0$, $R_I \geq 0$, and $R_S \geq 0$, we can conclude as follows:

$$R_V = 0, \quad R_I = 0, \quad R_S = 20 \quad (6)$$

In other words, rf-sputtering seems to produce an interfacial region having a significant thermal resistance ($(20 \pm 4.5) \times 10^{-9} \text{ m}^2 \cdot \text{K} \cdot \text{W}^{-1}$) between the gold film and the thermally oxidized SiO₂ film due to its high molecular energy on sputtering, but evaporation produces no such interfacial region, and as a result, the interfacial thermal resistance between the gold film and the thermally oxidized SiO₂ film is very small (less than $\pm 4.5 \times 10^{-9} \text{ m}^2 \cdot \text{K} \cdot \text{W}^{-1}$).

Results of the interfacial thermal resistances between the thermally oxidized SiO₂ film and the silicon wafer determined in this study are listed in Table 3. The VAMAS TWA23 data in Table 3 was corrected from the original data using the interfacial thermal resistance R_S estimated in this study. Both data in Table 3 show quite similar results in that the apparent interfacial thermal resistances between the thermally oxidized SiO₂ film and the silicon wafer scattered significantly ($\pm 9 \times 10^{-9} \text{ m}^2 \cdot \text{K} \cdot \text{W}^{-1}$) around a very small thermal resistance (less than $\pm 4.5 \times 10^{-9} \text{ m}^2 \cdot \text{K} \cdot \text{W}^{-1}$). It seems that the scatter of the data was due to the spatial distribution of the apparent interfacial thermal resistances on the plane of the silicon wafer. Such scatter of the apparent interfacial thermal resistance could occur, if a very thin interfacial region (<20 nm) of the thermally oxidized SiO₂ film was defective or crystallized [10].

5 Summary

- (1) This method can determine the thermal conductivity of an electrically insulating thin film with high accuracy.
- (2) This method requires simple preparation of the specimen in comparison with the three-omega method [4].
- (3) This method was verified by measurements of the thermally oxidized SiO₂ films (20 nm to 1,000 nm thick) on a silicon wafer including those used for the NIST Round Robin held in 1998. These results of the thermal-conductivity measurements coincide with those of VAMAS TWA23 (NIST Round Robin Report) within $\pm 4\%$.
- (4) Rf-sputtering seems to produce a significant thermal resistance ($(20 \pm 4.5) \times 10^{-9} \text{ m}^2 \cdot \text{K} \cdot \text{W}^{-1}$) between the gold film and the thermally oxidized SiO₂ film.
- (5) Evaporation seems to produce no significant interfacial thermal resistance (less than $\pm 4.5 \times 10^{-9} \text{ m}^2 \cdot \text{K} \cdot \text{W}^{-1}$) between the gold film and the thermally oxidized SiO₂ film.
- (6) The interfacial thermal resistances between the thermally oxidized SiO₂ film and the silicon wafer were found to scatter significantly ($\pm 9 \times 10^{-9} \text{ m}^2 \cdot \text{K} \cdot \text{W}^{-1}$) around a very small thermal resistance (less than $\pm 4.5 \times 10^{-9} \text{ m}^2 \cdot \text{K} \cdot \text{W}^{-1}$).

References

1. S.M. Lee, D.G. Cahill, *J. Appl. Phys.* **81**, 2950 (1997)
2. R. Kato, I. Hatta, in *Proceedings of 23rd Japan Symposium on Thermophysics Properties*, Tokyo, 2002, pp. 265–267
3. R. Kato, I. Hatta, in *Proceedings of 24th Japan Symposium on Thermophysics Properties*, Okayama, 2003, p. 258
4. R. Kato, I. Hatta, *Int. J. Thermophys.* **26**, 179 (2005)
5. A. Feldman, Results of a Round Robin on Thin Film Thermal Conductivity. Presented at 14th Symposium on Thermophysical Properties, Boulder, Colorado, 2000
6. A. Feldman, VAMAS TWA23 (2000)
7. R. Kato, A. Maesono, I. Hatta, in *Proceedings of 21st Japan Symposium on Thermophysics Properties*, Nagoya, 2000, pp. 10–12
8. R. Kato, A. Maesono, R.P. Tye, *Int. J. Thermophys.* **22**, 617 (2001)
9. R. Kato, I. Hatta, in *Proceedings of 25th Japan Symposium on Thermophysics Properties*, Nagano, 2004, p. 336
10. I. Takahashi, K. Nakano, J. Harada, T. Shimura, M. Umeno, *Surf. Sci.* **315**, L1021 (1994)